Supporting Information

Toxicological investigation of mycotoxin contaminants and antibiotic residues associated with the poultry industry and their impact on human health

Jahida Akter [a,b], Kabir Hossain [a,c], Santanu Deb Nath [a,d], Hozzatul Islam [a,c], Khaleda Afrin [a,e], Hamida Begum [a,f], Monir Uzzaman [a,e]*

[a] *Department of Toxicology Research, Computer in Chemistry and Medicine Laboratory, Dhaka, Bangladesh*
[b] *Department of Textile Engineering, Port City International University, Chittagong, Bangladesh*
[c] *Faculty of Science, Department of Applied Chemistry and Chemical Engineering, University of Chittagong, Chittagong, 4331, Bangladesh*
[d] *Faculty of Biological Sciences, Department of Biochemistry and Molecular Biology, Noakhali Science and Technology University, Noakhali-3814, Chittagong, Bangladesh*
[e] *Faculty of Science, Department of Chemistry, University of Chittagong, Chittagong, 4331, Bangladesh*
[f] *National Drug Control Laboratory, Dhaka, Bangladesh*

**Correspondence:* monircu92@gmail.com

Table of Contents

Table S1 Molecular formula (MF), molecular weight (MW), and enthalpy of all compounds.

Name	MF	MW (g/mol)	Enthalpy (Hartree)
ZER	$C_{18}H_{22}O_5$	318.40	-1074.94
AB1	$C_{17}H_{12}O_6$	312.27	-1106.09
CIP	$C_{17}H_{18}FN_3O_3$	331.34	-1148.05
ENR	$C_{19}H_{22}FN_3O_3$	359.40	-1226.62
OXY	$C_{22}H_{24}N_2O_9$	496.50	-1638.84
OTA	$C_{20}H_{18}ClNO_6$	403.80	-1738.97

Table S2 Energy (eV) of HOMO, LUMO, gap, hardness (η), softness (S), chemical potential (μ), electronegativity (χ), and electrophilicity (ω) of all toxic compounds.

Name	HOMO	LUMO	Gap	η	S	μ	χ	ω
ZER	-5.88	-1.25	4.63	2.32	0.22	-3.57	3.57	2.75
AB1	-6.09	-1.99	4.10	2.05	0.24	-4.04	4.04	3.98
CIP	-5.69	-1.20	4.49	2.25	0.22	-3.45	3.45	2.65
ENR	-5.69	-1.20	4.49	2.25	0.22	-3.45	3.45	2.65
OXY	-5.90	-1.80	4.10	2.05	0.24	-3.85	3.85	3.61
OTA	-6.39	-1.88	4.51	2.26	0.22	-4.12	4.12	3.79

Table S3 Different convergence parameters of all selected compounds.

Name	Maximum Force (meV/Å)	TL (meV/Å)	RMS Force (meV/Å)	TL (meV/Å)	MD (mÅ)	TL (mÅ)	RD (mÅ)	TL (mÅ)
ZER	0.72	23.14	0.21	15.43	0.30	0.95	0.08	0.63
AB1	0.62		0.10		0.49		0.09	
CIP	1.13		0.21		0.52		0.12	
ENR	0.36		0.10		0.64		0.11	
OXY	2.32		0.46		0.88		0.17	
OTA	0.87		0.15		0.89		0.21	

Threshold limit (TL), Maximum displacement (MD), RMS displacement (RD)

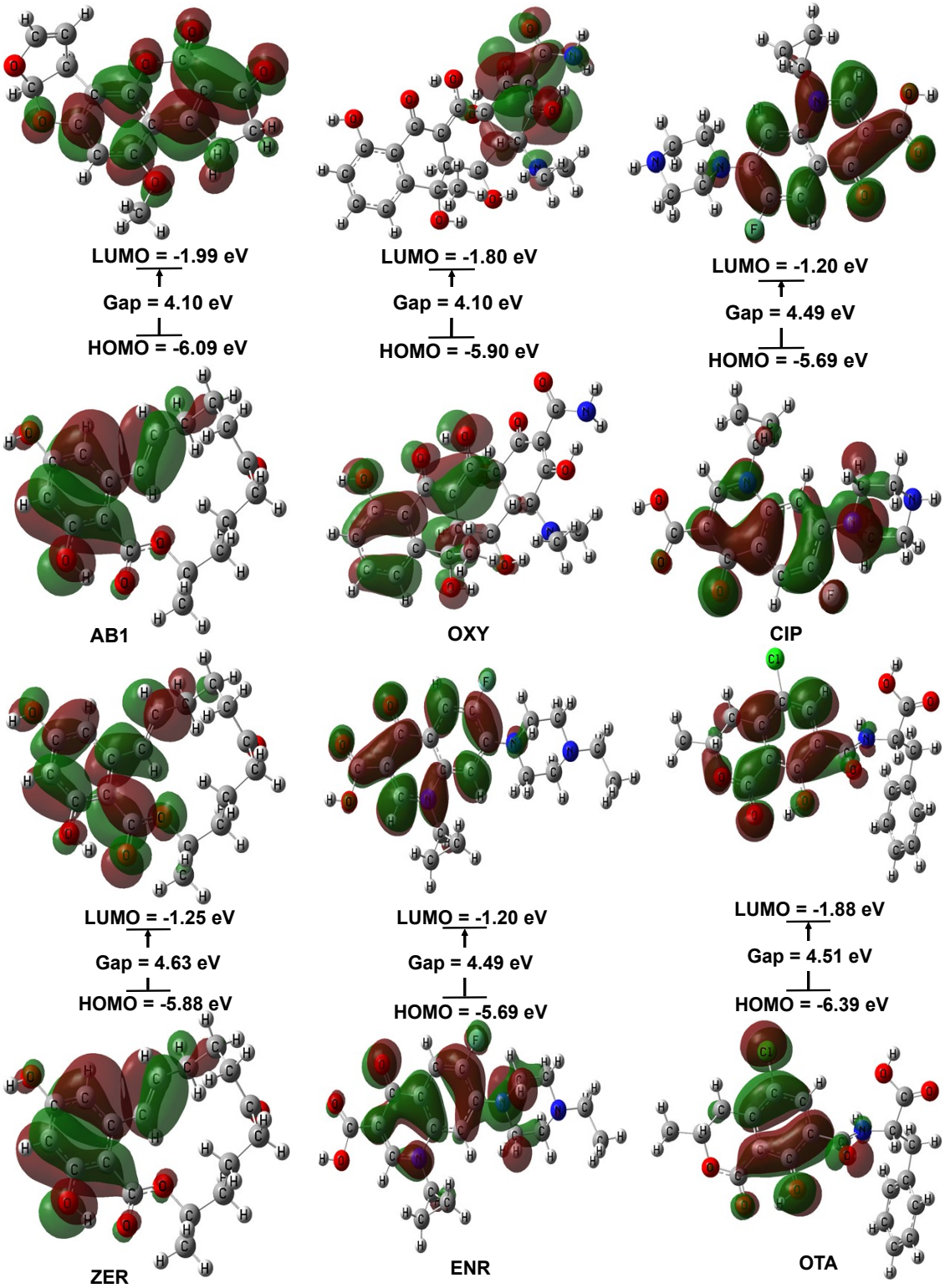

Fig. S1 Molecular orbital distribution of HOMO and LUMO energy states in the ground state of all compounds.

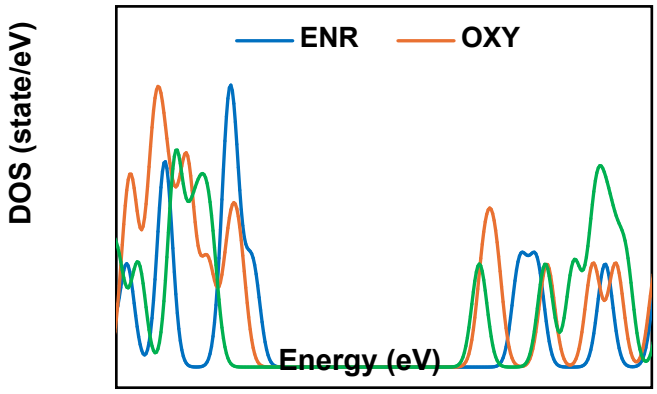

Fig. S2 DOS of ENR, OXY, and OTA (remaining compounds).

1.0. Active site selection

The selection of the active site was conducted using the 3D structure of selected proteins with the P2Rank binding pocket prediction algorithm, which helped to analyze the protein's surface geometry. Pocket 1 was identified as the most probable active site [1]. The probability was 0.95 and 0.98, indicating a true binding site for the 4G1C and 3P0M proteins, respectively, while the probability of the 2RJQ protein was 0.71. The number of residues was 17 (for 2RGQ), 37 (for 4G1C), and 31 (for 3P0M), suggesting a well-defined pocket, with these residues forming a deep cavity. The decent conservation scores were 2.20 (for 2RJQ), 2.01 (for 4G1C), and 2.65 (for 3P0M), supporting its functional relevance as a ligand-binding region. The identified active site region was visualized in red on the protein surface, representing the most probable ligand-binding cavity, illustrated in **Fig. S3**.

2.0. Docking validation

The stereochemical quality of the selected protein was evaluated using the Ramachandran plot, which was generated by PROCHECK [2]. The results showed that 88.8% of residues were in the most favored regions, 10.4% in additional allowed regions, and only 0.4% in disallowed regions for the 2RJQ protein. While 91.0% residues were in the most favored regions, 8.5% in additional allowed regions, and no residues were available in disallowed regions for the 4G1C protein. Furthermore, 91.9% of residues were in the most favored regions, 8.1% in additional allowed regions, and no residues were available in disallowed regions

for the 3P0M protein, illustrated in **Fig. S4(a)**, **(b)**, and **(c),** respectively. Since a good-quality protein structure is expected to have >90% residues in the most favored regions and <1% in disallowed regions, the structure can be considered reliable for subsequent molecular docking and MD simulation studies [3].

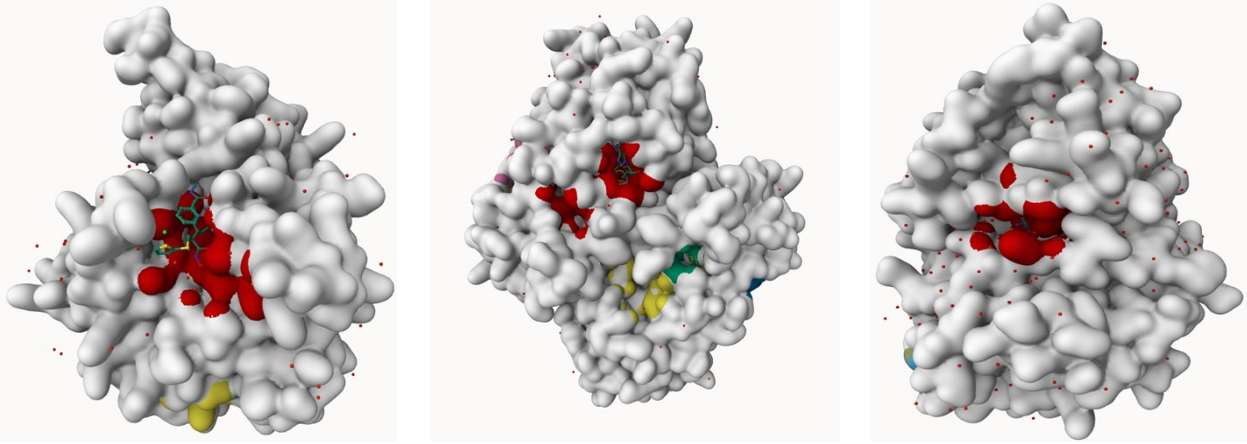

Fig. S3 Predicted active site of **(a)** 2RJQ, **(b)** 4G1C, and **(c)** 3P0M proteins showing the top-ranked binding pocket (in red) identified by structure-based pocket prediction.

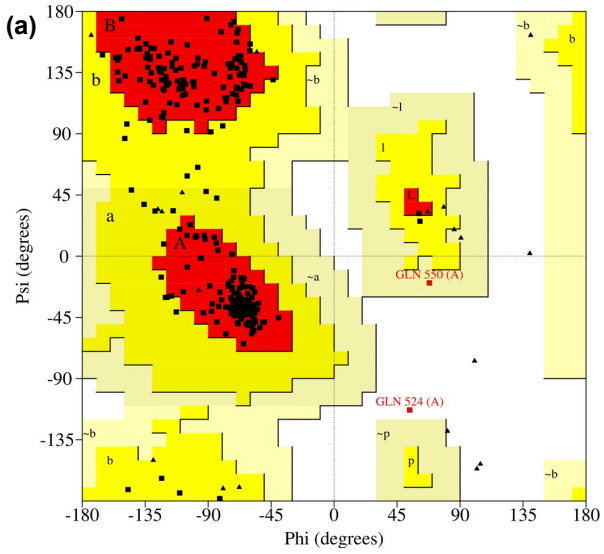

Plot statistics

Residues in most favoured regions [A,B,L]	230	88.8%
Residues in additional allowed regions [a,b,l,p]	27	10.4%
Residues in generously allowed regions [~a,~b,~l,~p]	1	0.4%
Residues in disallowed regions	1	0.4%
Number of non-glycine and non-proline residues	259	100.0%
Number of end-residues (excl. Gly and Pro)	3	
Number of glycine residues (shown as triangles)	22	
Number of proline residues	9	
Total number of residues	293	

Based on an analysis of 118 structures of resolution of at least 2.0 Angstroms and R-factor no greater than 20%, a good quality model would be expected to have over 90% in the most favoured regions.

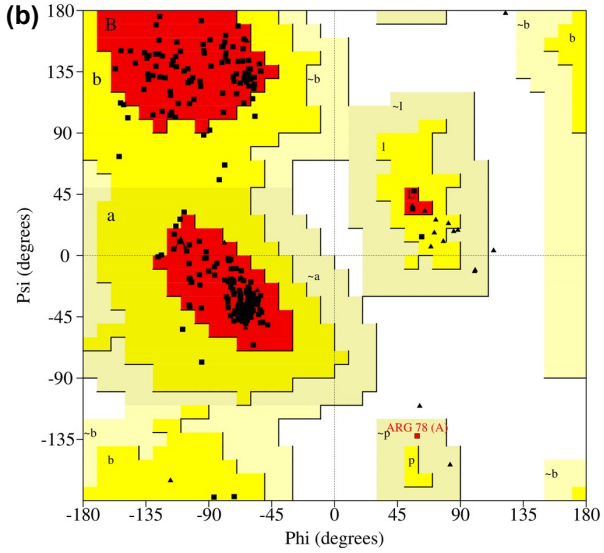

Plot statistics

Residues in most favoured regions [A,B,L]	203	91.0%
Residues in additional allowed regions [a,b,l,p]	19	8.5%
Residues in generously allowed regions [~a,~b,~l,~p]	1	0.4%
Residues in disallowed regions	0	0.0%
Number of non-glycine and non-proline residues	223	100.0%
Number of end-residues (excl. Gly and Pro)	2	
Number of glycine residues (shown as triangles)	24	
Number of proline residues	19	
Total number of residues	268	

Based on an analysis of 118 structures of resolution of at least 2.0 Angstroms and R-factor no greater than 20%, a good quality model would be expected to have over 90% in the most favoured regions.

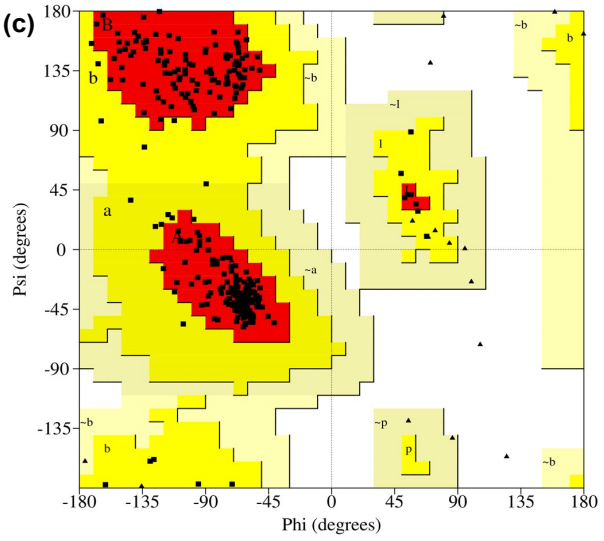

Plot statistics

Residues in most favoured regions [A,B,L]	271	91.9%
Residues in additional allowed regions [a,b,l,p]	24	8.1%
Residues in generously allowed regions [~a,~b,~l,~p]	0	0.0%
Residues in disallowed regions	0	0.0%
Number of non-glycine and non-proline residues	295	100.0%
Number of end-residues (excl. Gly and Pro)	7	
Number of glycine residues (shown as triangles)	20	
Number of proline residues	14	
Total number of residues	336	

Based on an analysis of 118 structures of resolution of at least 2.0 Angstroms and R-factor no greater than 20%, a good quality model would be expected to have over 90% in the most favoured regions.

Fig. S4 Ramachandran plot of the **(a)** 2RJQ, **(b)** 4G1C, and **(c)** 3P0M generated by PROCHECK.

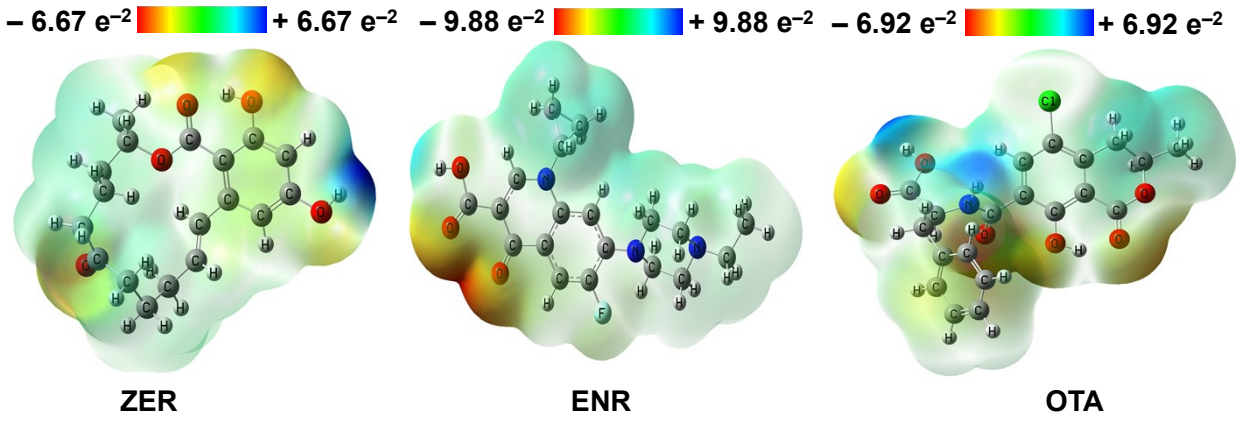

Fig. S5 Molecular electrostatic potential (MEP) map of selected compounds.

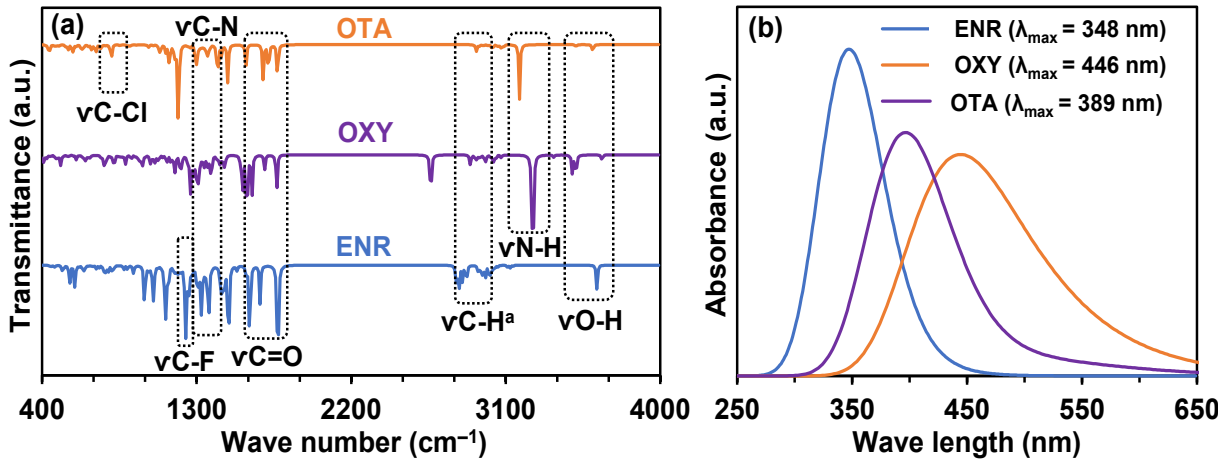

Fig. S6 (a) FT-IR and **(b)** UV-visible spectra of selected compounds.

Table S4 Vibrational frequencies of all compounds.

Compounds	Assignment	Frequency (scaled, cm^{-1})	Frequency (experimental, cm^{-1})
ZER	$\nu C{=}O^{s}$	1729	1715-1720
	$\nu C\text{-}H^{s}$	2900	--
	$\nu C\text{-}H^{as}$	2974-3017	--
	$\nu C\text{-}C^{a}$	1572-1598	1580-1590
	$\nu O\text{-}H^{s}$	3133-3673	--
	$\nu C{=}O^{s}$	1729-1810	1706
	$\nu C\text{-}H^{s}$	2919	--

AB1	vC-H^{as}	2956-3136	2853-2925
	vC-C^{a}	1541-1634	--
CIP	vC-C^{a}	1609	--
	vC-N^{a}	1329	--
	vC-N	1260	--
	vC=O	1669-1772	1700-1750
	vC-H^{as}	2964-3142	2950-3000
	vO-H	3630	3450-3500
	vN-H	3397	--
	vC-F ^{a}	1240	--
ENR	vC-N^{a}	1329	--
	vC=O^{s}	1669-1772	1737
	vC-H^{as}	3004	--
	vC-H^{s}	2810-2937	--
	vC-H^{a}	3110	--
	vO-H^{s}	3631	3300-3500
	vC-F	1237	--
OXY	vN-H^{s}	3377	--
	vO-H	3488-3661	--
	vC=O	1695-1765	1621
	vC-N^{a}	1317	1218
	vC-H^{s}	2925	--
	vC-H^{as}	2985	--
OTA	vO-H	3608	3380
	vN-H	3509	--
	vO-H	3180	--
	vC-H^{as}	3076-3088	--
	vC-H^{s}	2915-2970	2988
	vC-Cl	713	--
	vC=O	1687-1771	1723
	vC-N^{a}	1242	1140

s = stretching, as = asymmetric, a = aromatic

Table S5 Electronic transition data of all compounds.

Name	Wavelength (nm)	Excited energy (eV)	Configuration composition (%)	Oscillator strength
AB1	315.23	3.93	H-3→L (75.46)	0.0721
CIP	347.48	3.57	H→L (86.21)	0.1012
ENR	347.97	3.56	H→L (80.96)	0.1022
OTA	396.10	3.13	H-1→L (96.27)	0.0810
OXY	431.49	2.87	H-1→L (63.49)	0.0047
ZER	325.96	3.80	H→L (90.05)	0.0952

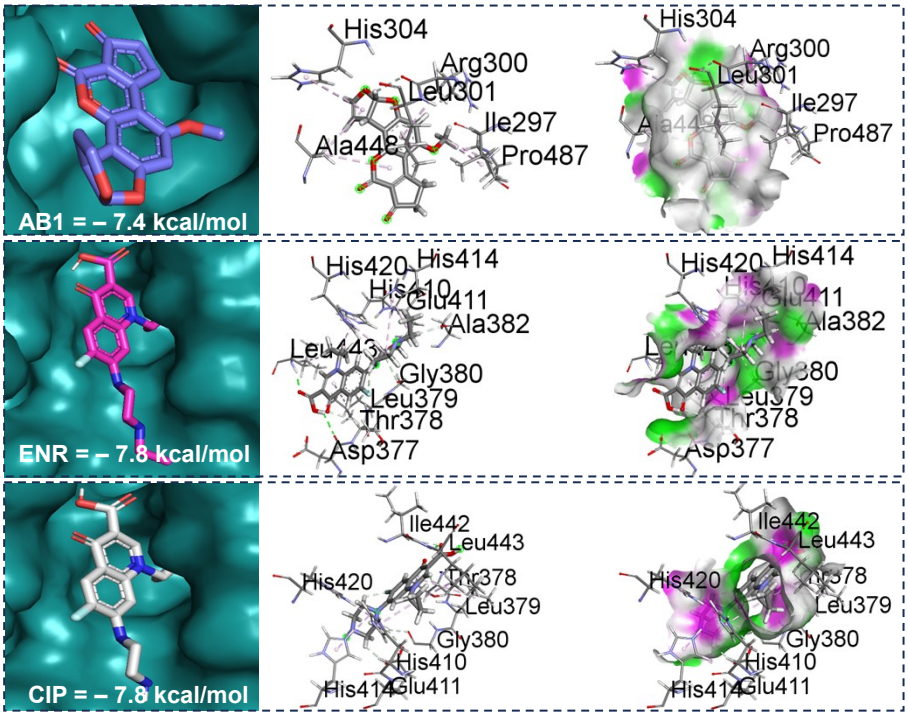

(a) PDB ID: 2RJQ

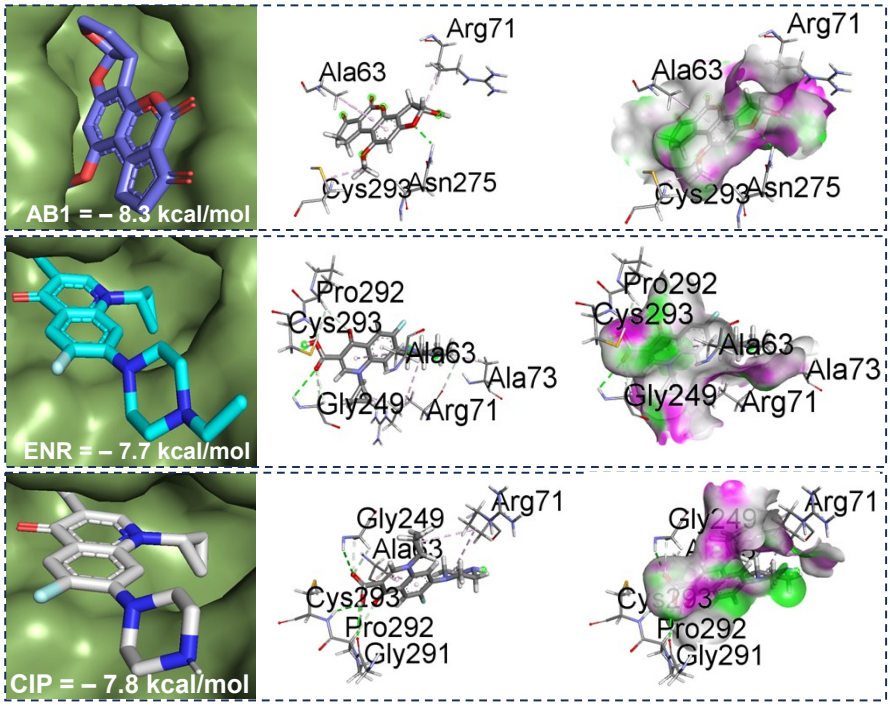

(b) PDB ID: 4G1C

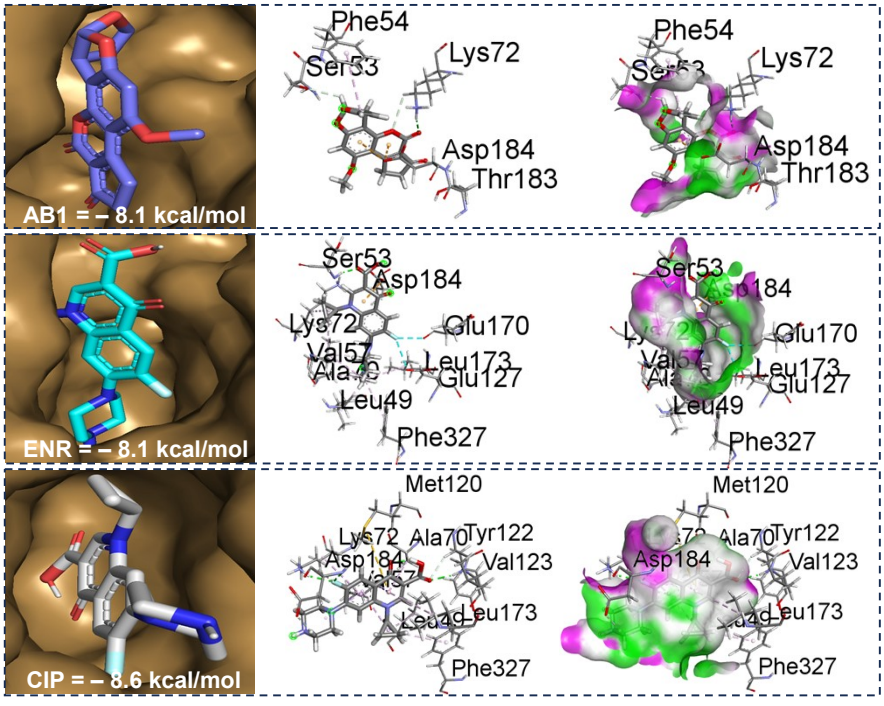

(c) PDB ID: 3P0M

Fig. S7 Superimposed docked conformers selected analogs within the active site of the receptor protein, nonbonding interactions, and hydrogen bond surface area of selected toxic compounds with receptor protein **(a)** 2RJQ, **(b)** 4G1C, and **(c)** 3P0M receptor proteins.

Table S6 Average binding affinities and nonbonding interactions of all compounds after molecular docking with receptor proteins 2RJQ, 4G1C, 3P0M.

Compounds	Residues in contact			Interaction type			Distance (Å)		
	2RJQ	4G1C	3P0M	2RJQ	4G1C	3P0M	2RJQ	4G1C	3P0M
ZER	LEU 443	SER 251	SER 53	H	H	H	1.99	2.48	2.69
	HIS 414	PHE 70	LYS 72	CHB	PPS	H	3.07	5.06	2.45
	ILE 442	ILE 142	LYS 72	CHB	A	CHB	2.51	4.42	2.54
	HIS 420	PHE 70	ASP 184	PC	PA	Pa	4.46	5.47	4.02
	HIS 420	HIS 158	LEU 74	PPT	PA	A	5.33	5.27	5.38
	--	ALA 59	PHE 54	--	PA	PA	--	4.82	4.43
	--	VAL 254	--	--	PA	--	--	5.24	
AB1	ARG 300	ASN 275	LYS 72	CHB	H	H	2.64	2.28	2.18
	ALA 448	ARG 71	LYS 72	A	A	CHB	4.34	3.84	3.09
	ILE 297	CYS 293	THR 183	A	A	CHB	4.25	3.60	2.92
	PRO 487	ALA 63	SER 53	A	PA	CHB	4.22	3.62	2.84
	HIS 304	ALA 63	ASP 184	PA	PA	Pa	5.41	4.91	3.40
	ALA 448	--	PHE 54	PA	--	PA	5.02	--	4.59
	ARG 300	--	--	PA	--	--	4.88	--	--
	LEU 301	--	--	PA	--	--	5.36	--	--
CIP	LEU 443	GLY 249	LYS 72	H	H	H	1.92	3.01	2.19
	THR 378	CYS 293	VAL 123	CHB	H	H	2.47	2.63	2.07
	ILE 442	GLY 291	ASP 184	CHB	H	H	2.87	2.50	2.85
	GLY 380	GLY 249	TYR 122	CHB	CHB	CHB	2.78	2.51	2.62

	GLU 411	PRO 292	ASP 184	CHB	CHB	CHB	2.53	2.72	2.48
	LEU 443	ARG 71	VAL 57	A	A	PS	4.75	4.67	2.72
	HIS 410	ALA 63	MET 120	PA	PA	Ps	3.74	3.78	5.82
	HIS 414	ALA 63	VAL 57	PA	PA	A	5.05	4.52	4.84
	LEU 379	--	LEU 49	PA	--	A	5.30	--	5.27
	--	--	PHE 327	--	--	PA	--	--	5.47
	--	--	LYS 72	--	--	PA	--	--	5.37
	--	--	ALA 70	--	--	PA	--	--	4.42
	--	--	LEU 173	--	--	PA	--	--	5.08
	LEU 443	GLY 249	SER 53	H	H	H	1.94	2.97	2.14
	ASP 377	CYS 293	GLU 127	H	H	F	2.47	2.58	3.32
	THR 378	GLY 249	GLU 170	CHB	CHB	F	2.53	2.50	2.97
	GLY 380	PRO 292	ASP 184	CHB	CHB	Pa	2.88	2.58	3.74
	GLU 411	ARG 71	VAL 57	CHB	CHB	A	2.66	3.06	3.93
ENR	ALA 382	ARG 71	ALA 70	CHB	A	A	2.14	5.19	4.48
	LEU 443	ALA 73	LYS 72	A	A	A	4.66	3.93	4.45
	HIS 410	ALA 63	LEU 49	PA	PA	A	3.79	3.70	4.12
	HIS 414	ALA 63	VAL 57	PA	PA	A	4.88	4.48	4.93
	HIS 420	--	LEU 173	PA	--	A	4.76	--	4.87
	LEU 379	--	PHE 327	PA	--	PA	5.26	--	4.66
	GLY 380	PHE 70	LYS 72	H	H	H	2.63	2.91	3.06
	CYS 371	ILE 142	LYS 168	H	H	H	2.89	2.73	2.35
OXY	THR 378	SER 251	THR 51	CHB	H	H	2.90	2.87	1.76
	HIS 373	GLN 140	ASP 184	CHB	H	H	2.75	2.05	2.36
	ALA 335	THR 69	GLU 127	PA	CHB	H	5.08	2.41	2.83

	--	ARG 105	LYS 168	--	PC	CHB	--	3.43	5.59
	--	ALA 59	ASN 171	--	PA	CHB	--	4.83	2.43
	--	ILE 142	THR 51	--	PA	CHB	--	5.04	2.70
	--	--	VAL 57	--		PS	--	--	2.92
OTA	LEU 379	ARG 105	PHE 54	H	H	H	1.94	2.05	2.58
	LEU 443	ILE 142	GLY 55	H	H	H	2.26	2.09	2.47
	SER 441	ALA 59	GLY 50	H	CHB	CHB	2.58	2.68	2.30
	GLY 380	ASN 141	THR 183	H	CHB	CHB	2.06	2.80	2.61
	ASP 377	ARG 105	ASP 184	CHB	CHB	Pa	2.80	2.52	4.09
	ASP 377	PHE 223	VAL 57	Pa	PS	A	3.18	2.74	3.94
	HIS 410	PHE 70	LEU 173	PPS	PPS	A	3.71	5.41	5.28
	ILE 442	HIS 158	LEU 49	A	PPS	A	4.71	5.55	4.66
	ILE 442	VAL 254	LYS 72	PA	A	A	3.91	4.67	4.91
	LEU 443	PHE 223	MET 120	PA	PA	A	4.49	4.40	4.89
	--	ILE 142	PHE 327	--	PA	PA	--	5.39	5.03
	--	VAL 67	VAL 57	--	PA	PA	--	4.39	4.48
	--	PRO 68	--	--	PA	--	--	5.46	--
	--	ARG 105	--	--	PA	--	--	4.01	--

H = conventional hydrogen bond, CHB = carbon hydrogen bond, PC = π cation, PPT = π-π T-shaped, A = alkyl, PA = π-alkyl, Pa = π-anion, PPS = π-π stacked, PHB = π-donor hydrogen bond, PS = π-sigma, Ps = π-sulfur, F = Fluorine.

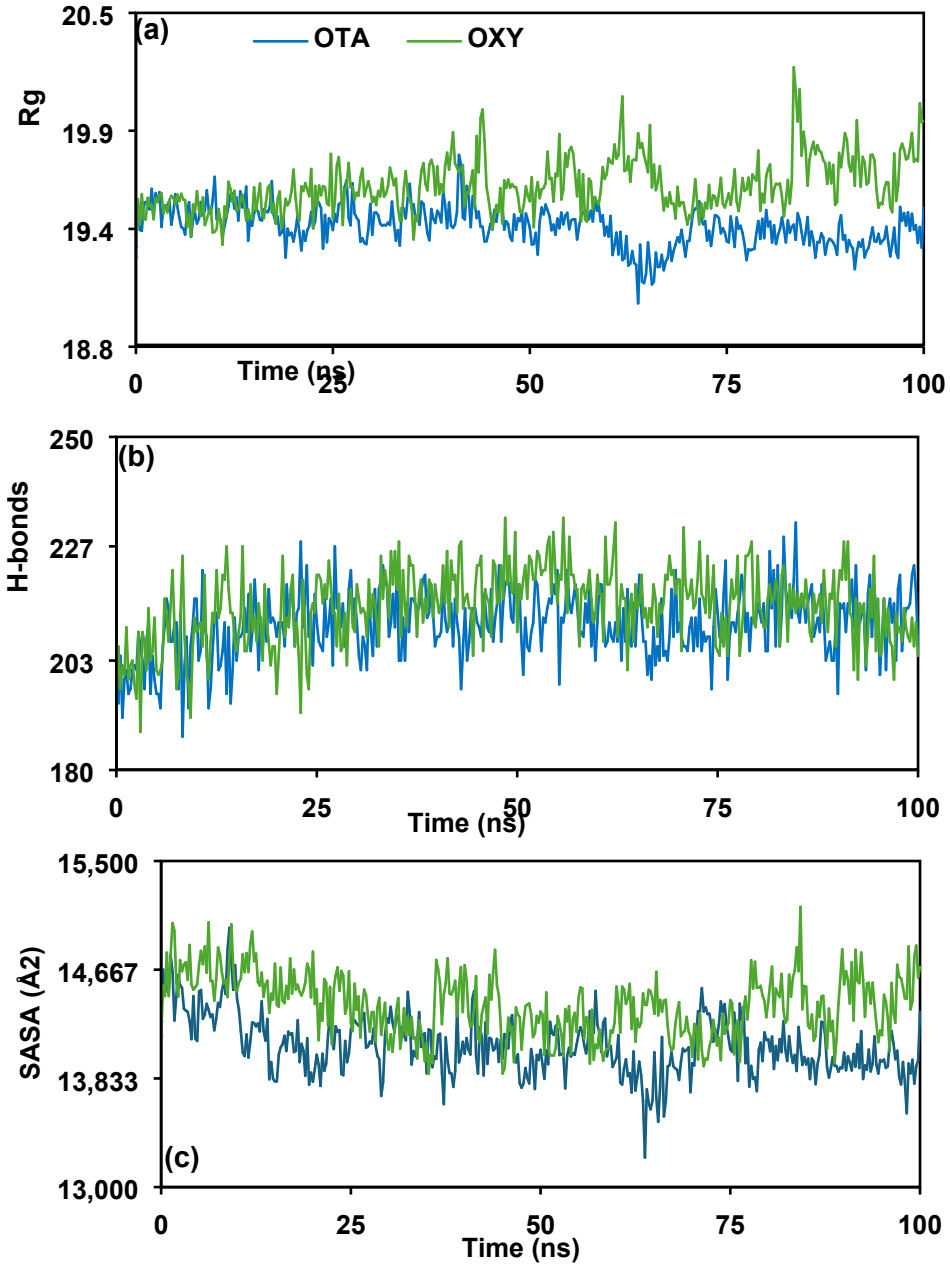

Fig. S8 (a) Rg, **(b)** H-bonds, and **(c)** SASA of the selected complexes during 100 ns MD simulation within the 2RJQ protein.

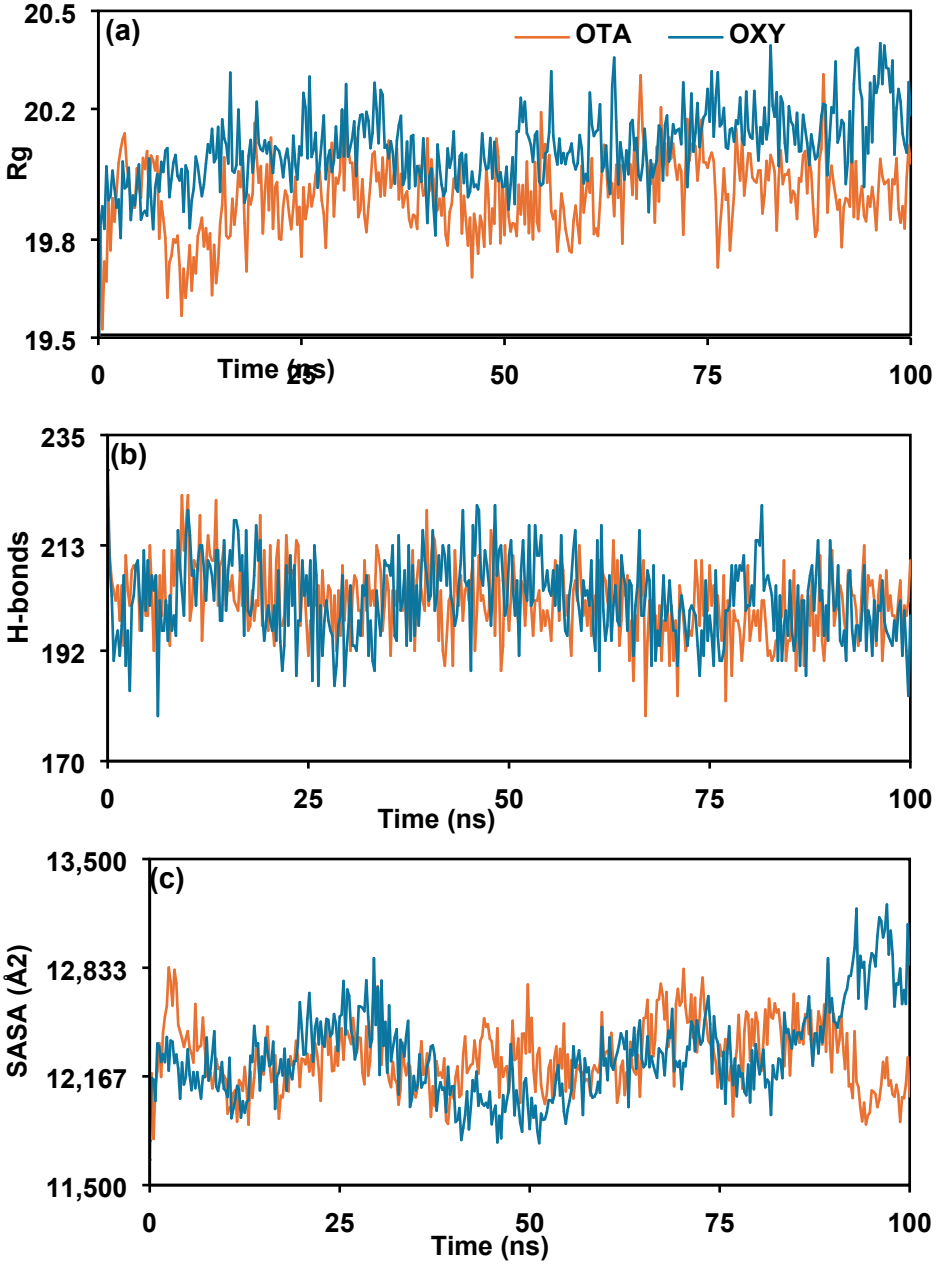

Fig. S9 (a) Rg, **(b)** H-bonds, and **(c)** SASA of the selected complexes during 100 ns MD simulation within the 4G1C protein.

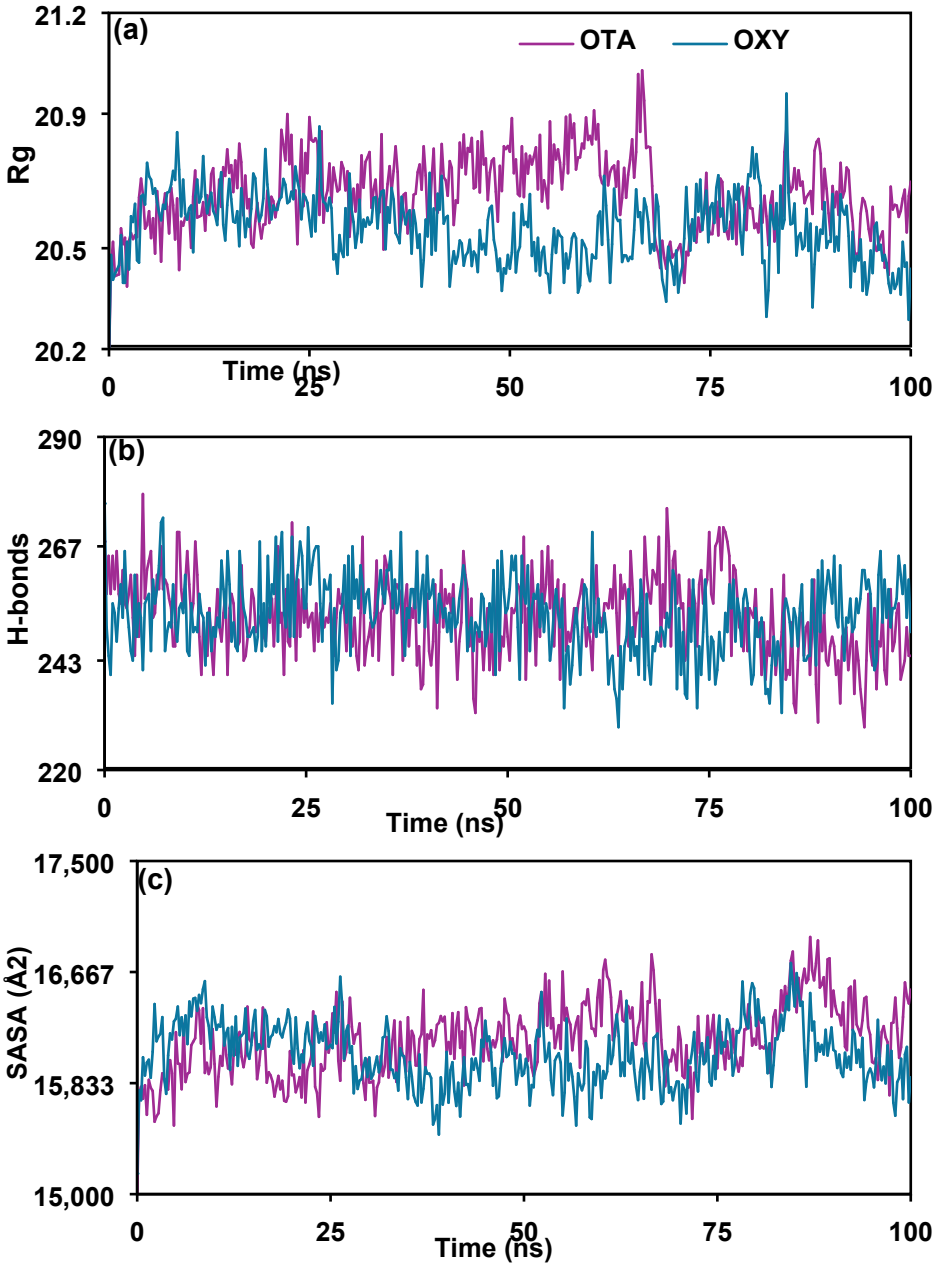

Fig. S10 (a) Rg, **(b)** H-bonds, and **(c)** SASA of the selected complexes during 100 ns MD simulation within the 3P0M protein.

Table S7. Quantitative structure-activity relationship study of toxic compounds.

Compounds	Chiv5	bcutm1	MRVSA9	MRVSA6	PEOEVSA5	GATSv4	J	Diameter	pIC_{50}
ZER	1.6	3.91	17.82	29.33	12.15	1.11	2.01	10	4.35
AB1	2.53	4.15	16.75	45.51	0	0.9	1.5	9	4.61
CIP	2.41	4.13	22.56	39.93	0	0.76	1.53	11	4.64
ENR	2.66	4.13	22.56	39.93	6.92	0.78	1.48	13	4.87
OXY	4.19	4.05	17.47	51.99	12.13	1.07	1.87	11	4.92
OTA	2.4	4.03	29.44	63.67	41.93	1.07	1.63	14	4.75

A multiple linear regression (MLR) equation was used to calculate the pIC_{50} values. The following formula is as follows:

pIC_{50} (Activity) = -2.77 + 0.14 × Chiv5 + 1.60 × bcutm1 + 0.02 × MRVSA9 + (-0.003) × MRVSA6 + 0.007 × PEOEVSA5 + -0.16 × GATSv4 + 0.21 × J + 0.08 × Diameter.

Note for **Table S7**:

Chiv5: A molecular descriptor representing the Chi molecular shape index, which measures the complexity of a molecule's shape in relation to the distribution of atoms. It provides insight into molecular flexibility or rigidity, which can influence bioactivity and molecular interactions.

bcutm1: A descriptor based on the BCUT (Biological Coarse-grained Unit Tensor) method, which quantifies molecular properties related to the graph structure of a molecule. It reflects symmetry and compactness, which are important for understanding molecular behavior and interactions.

MRVSA9: Molecular Refractivity and Volume Surface Area descriptor, which measures the volume and surface area of a molecule. It is often used to evaluate how the size and shape of a molecule affect its bioavailability and interaction with biological targets.

MRVSA6: Another MRVSA index that is based on the surface area of a molecule. This descriptor helps assess how molecular size, shape, and surface area influence the compound's potential for interaction with receptors or biomolecules, which is critical for drug design.

PEOEVSA5: Partial Electrostatic Surface Area (PEOEVSA) descriptor, representing the distribution of electrostatic potential across the molecule's surface. It helps in evaluating the molecule's polarity and its potential to interact with biological receptors, providing insights into solubility and bioactivity.

GATSv4: Geary's Autocorrelation of the lagged molecular property (v4) descriptor, which measures the spatial distribution of molecular properties (like charge or dipole moment) across the entire molecule. It helps us understand how different parts of a molecule interact spatially, which is crucial for predicting biological activity.

J: The Jaccard Similarity Coefficient. This measures the similarity between two sets (in this case, molecular descriptors). It is used to compare molecules and evaluate their structural similarities, often applied in virtual screening or similarity-based drug design.

Diameter: Refers to the diameter of the molecule, which is the largest distance between any two atoms in the molecule. This descriptor is a measure of the molecule's size and compactness, which is important in understanding how a molecule fits into binding sites and interacts with receptors.

pIC_{50}: The negative logarithm of the IC50 value (in mol/L), where IC_{50} represents the concentration of a compound required to inhibit 50% of a biological activity. A higher pIC_{50} value indicates greater potency and is used as an indicator of the compound's effectiveness in inhibiting a specific biological function [4].

References

1 R. Krivák and D. Hoksza, Predicting protein-ligand binding sites using deep convolutional neural networks, *J Cheminform.*, 2018, **10**, 1–12.

2 Z. Amiri, M. Bayat and D. Gheidari, Synthesis of thiazoloquinolinone derivatives: molecular docking, MD simulation, and pharmacological evaluation as VEGFR-2 inhibitors, *BMC Chem*, 2025, **19**, 1–24.

3 O. V. Sobolev, P. V. Afonine, N. W. Moriarty, M. L. Hekkelman, R. P. Joosten, A. Perrakis and P. D. Adams, Synthesis of thiazoloquinolinone derivatives: molecular docking, MD simulation, and pharmacological evaluation as VEGFR-2 inhibitors, *Structure*, 2020, **28**, 1249-1258.e2.

4 M. O. Farque, R. M. Islam, M. F. Rahman Joni, M. Akter, S. Akter, M. D. Islam, M. J. Bin Salim, A. A. Aziz, E. Kabir and M. Uzzaman, Structural modification of Naproxen; physicochemical, spectral, medicinal, and pharmacological evaluation, *Inform. Med. Unlocked*, 2025, **53**, 101617.